J Mol Model (2011) 17:2989–2994
DOI 10.1007/s00894-011-1019-2

ORIGINAL PAPER

Structural phase transition of SnSe under uniaxial stress and hydrostatic pressure: an *ab initio* study

Sebahaddin Alptekin

Received: 29 December 2010 / Accepted: 9 February 2011 / Published online: 1 March 2011

Abstract We study the structural behavior of SnSe under the hydrostatic pressure using a constant pressure *ab initio* technique. We find SnSe undergoes a structural second order phase transition from the orthorhombic (*Pnma*) structure to orthorhombic (*Cmcm*) structure in the constant pressure simulation at 7 GPa which is in good agreement with the recent experimental study. The *Cmcm* structure is fivefold coordinated. This phase transition is also analyzed from the total energy calculations. Besides, we study the behavior of SnSe under uniaxial stress.

Keywords *Ab initio* calculation · Phase transformation · Semiconductors · Uniaxial stress

Introduction

Two dimensional layered group IV-VI compounds have remarkable electronic and optical properties; so, they have various potential applications in optoelectronic devices. In order to understand their physical properties and pressure-induced phase transitions, considerable effort has been made in the past few years [1–8]. However, many unknowns and controversies about the presence or absence of the phase transitions in some of these compounds still exist. Although the reason of these controversies is undetermined, cause of these controversies may be the sample's properties, pressurizing techniques and the degree of hydrostatic pressure.

SnSe, a typical example of two dimensional layered group IV-VI compounds, has a layered orthorhombic structure with the *Pnma* space group. The unit cell consists of two-layers, and atoms within the layers are covalently bonded to three neighbors (see Fig. 1). The layers pile up with a weak van der Walls-like coupling along *a*-direction. The limited information about the high pressure phase of SnSe stimulates us to explore its behavior under hydrostatic pressure using an *ab initio* constant pressure technique. Initially, a gradual phase transformation from Pnma to Cmcm at high pressure is predicted through the simulations. Our results might offer the opportunity to better understand the behavior of SnSe and the other two dimensional layered structures under pressure.

SnSe is a orthorhombic crystal with eight atoms per unit cell and lattice parameters a=4.46 , b=4.19 and c=11.57 Å [9]. The Sn and Se atoms form double layers made up of two planes of zigzag Sn-Se chains perpendicular to the longest axis. Each atom has the coordination environment of a heavily distorted octahedron and the lattice can be thought of as a deformed NaCl type [10].

Peters and McNeil [11] studied the high-pressure behavior of SnSe, which is isostructural to α-SnSe (Pnma), up to 14 GPa using ^{119}Sn Mössbauer spectroscopy. In increasing pressure between 1.4 GPa and 3 GPa, the pronounced changes in the isomer shift, the quadrupole splitting and the effective thickness of the sample were found. The observed changes above 3 GPa were significantly smaller. The authors attribute this behavior to the rapid change of interlayer distances at lower pressures and the small changes of the intralayer distances in the high-pressure region.

S. Alptekin (✉)
Department of Physics, Faculty of Science, Cankiri Karatekin University,
18100 Cankiri, TURKEY
e-mail: salptekin@karatekin.edu.tr

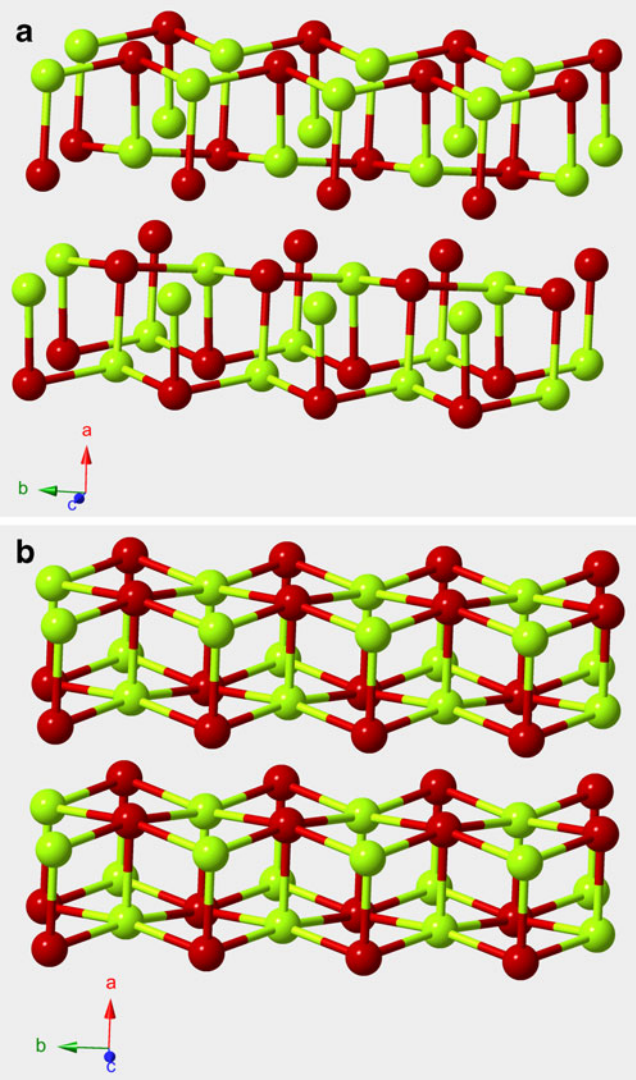

Fig. 1 Crystal structures of SnSe (**a**) the Pnma phase at zero-pressure and (**b**) the Cmcm phase of SnSe formed at 7 GPa (The atoms Sn and Se have red and green colors, respectively)

Methods

We used the first-principles pseudopotential method within the density functional theory (DFT) and the generalized gradient approximation (GGA) of Perdew-Burke and Ernzerhof for the exchange-correlation energy [12]. The calculation was carried out with the *ab initio* program SIESTA [13] using a linear combination of atomic orbitals as the basis set, and the norm-conservative Troullier-Martins Pseudopotentials [14]. Double-ξ, plus polarized basis sets were employed. A uniform mesh with a plane wave cut-off of 150 Ry was used to represent the electron density the local part of the pseudopotentials, and the Hartree and the exchange-correlation potential. The simulation cell consists of 64 atoms with periodic boundary conditions. We used Γ-point sampling for the Brillouin zone integration. The system was first equilibrated at zero pressure, and then pressure was gradually increased. For each value of the applied pressure, the structure was allowed to relax and find its equilibrium volume and the lowest energy by optimizing its lattice vectors and atomic positions together until the stress tolerance was less than 0.5 GPa and the maximum atomic force was smaller than 0.01 eV·Å^{-1}. For the minimization of geometries, a variable-cell shape conjugate- gradient method under a constant pressure was used. For the energy volume calculations, we considered the unit cell for SnSe phases. The Brillouin zone integration was performed with an automatically generated 10x10x10 k-point mesh for the phases following the convention of Monkhorst and Pack [15]. In order to determine the symmetry of the high pressure phases formed in the simulations, we used the KPLOT program [16] that provides detailed information about the space group, the cell parameters and the atomic position of a given structure. For the symmetry analysis we used 0.2 Å, 4°, and 0.7 Å tolerances for the bond length, bond angles and inter planar spacing, respectively.

Constant pressure *ab initio* calculation

We first compare our calculated lattice parameters with variable experimental data for the *Pnma* phase of SnSe [11]. The equilibrium unit cell lattice constants of SnSe are found to be a=11.69 Å, b=4.23 Å and c=5.52 Å. These values are comparable with the experimental results of a= 11.57 Å, b=4.19 Å and c=4.46 Å [9]. The SnSe structure has two distinct bond lengths of 2.82 Å and 2.84 Å at ambient pressure. These values are in agreement with the experimental results of 2.77-2.82 Å [11]. The nearest nonbonding distance between atoms in different layers is 3.41 Å. The experimental value of this separation is 3.35 Å [11]. Starting from the zero-pressure structure, we gradually increase the pressure and carefully analyze the structure of SnSe at each applied pressure using the KPLOT program. At 7 GPa, we find a phase transformation into an orthorhombic structure with space group *Cmcm* with eight atoms per unit cell. Its lattice parameters are a=4.16 Å, b= 11.16 Å and c=4.14 Å and its atomic positions are Sn:(0, 0.883858, 0.25) and Se:(0, 0.638389, 0.25). The structure consists of rocksalt-like bilayers, stacked along the b axis of the orthorhombic unit cell. Each Sn and Se atoms have five unlike neighbors but the Sn-Se bonding do not have the same bond lengths on all sites. Both Sn and Se have four neighbors at 2.74 Å in the b–c planes and one neighbor at 2.95 Å perpendicular to the layer planes. The closest Sn…Sn and Se…Se neighbor separation are about 4.14 and 4.16 Å, respectively. The variation of the simulation cell vectors as a function of pressure might provide valuable information about this phase transformation. Figure 2

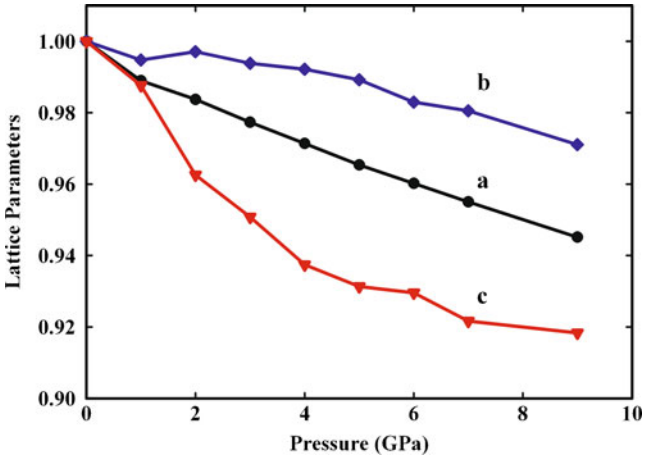

Fig. 2 Pressure dependence of the lattice parameters (The y axis contains normalized values)

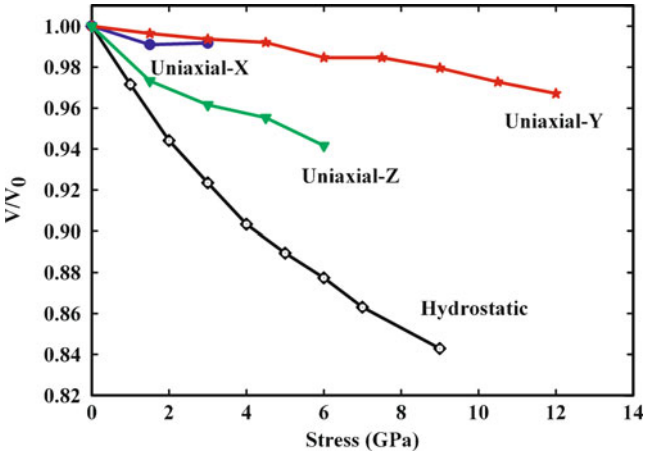

Fig. 3 Volume change as a function of hydrostatic pressure and uniaxial stress

shows the cell lengths as a function of the applied pressure. This implies that the main compression mechanism of SnSe is the significant shortening along the puckered layers. Similar behavior was determined in the previous studies of isostructural GeS [3, 8] and GeSe [2, 4]. This trend, however, is quite different from the other layer-like chalcogenides such as SnS_2 [17] and TiS_2 [18] in which the strongest compression occurs along the weak interlayer direction. It is also noteworthy here that the simulation cell angles remain 90° during the phase transformation and hence this phase change is not associated with shear deformation. To investigate the structural changes through the transition further, we studied the variation of the first neighbor Sn-Se bond lengths with pressure. The SnSe structure has two distinct bond lengths at ambient pressure. From these observations, we conclude that the major compression mechanism of SnSe is due to the narrowing of the intralayer and interlayer separations and the bond bending. Figure 3 indicates that the volume changes as a function of hydrostatic pressure and uniaxial stress in SnSe.

Uniaxial stress

Besides the hydrostatic pressure, studies of the structural and mechanical responses of materials at finite strain are crucial for our understanding of many areas such as phase transformation, theoretical strength, crack propagation and nanotechnology. There are not any studies that explore the behavior of SnSe under a uniaxial stress. The lack of such information stimulates us to investigate systematically the stability of SnSe subjected to a uniaxial stress. We apply compressive stresses [100], [010] and [001] directions. The volume change as a function of uniaxial stress is also given in Fig. 3. As seen from the figure, the volume decreases with increasing compressive uniaxial stress but the change in the volume is quite less than that of hydrostatic case as expected. SnSe exhibits structural failure at 3 GPa and 14 GPa in our simulation. Certainly, these critical stresses are overestimated in the simulation as being the hydrostatic case. We cannot however absolutely tell the degree of the overestimation of these critical stresses in the simulation because we are not aware of any experimental studies on the behavior of SnSe under uniaxial stresses but we suppose that they are a factor of 6–8 times larger than the experimental values as being the hydrostatic compression and hence we expect to see the structural failure of SnSe between 1.4 GPa and 3 GPa in experiments [11]. The axis compressed decreases gradually while the others tend to increase because the structure attempts to converse its volume. The simultaneous construction and expansions of the cell lengths change the structure from cubic to tetragonal without causing any coordination modification. A uniaxial compression of a solid usually yields an expansion in the transfer directions. Uniaxial stress and phase transition is given in Table 1. When uniaxial stress is applied, in x and y-directions no phase transition to *Cmcm* happened, but in z-direction, at 3 GPa pressure, phase transition to *Cmcm* came about. On the other hand, when hydrostatic pressure is applied, phase transition to *Cmcm* occurred at 7 GPa. So, stress applied in z-direction is the most convenient for this material in order to obtain phase transition.

Enthalpy calculations

There are generally overestimations for transition pressures in constant pressure simulations analogous to superheating molecular-dynamics simulations. This implies a high intrinsic activation barrier for transforming one solid phase into another in simulations. When the particular conditions such as finite size of simulation cells and the lack of any defect and surfaces in simulated structures are considered,

Table 1 Pressure and uniaxial stress dependence of the phase transition

Uniaxial stress	x-direction	y-direction	z-direction
Pressure(GPa)	Phase	Phase	Phase
0	Pnma	Pnma	Pnma
1.5	Pnma	Pnma	Pnma
3	Pnma	Pnma	Cmcm
4.5	P-1	Pnma	Cmcm
6		Pnma	Cmcm
7.5		Pnma	P1
9		Pnma	
10.5		Pnma	
12		Pnma	
13.5		P-1	

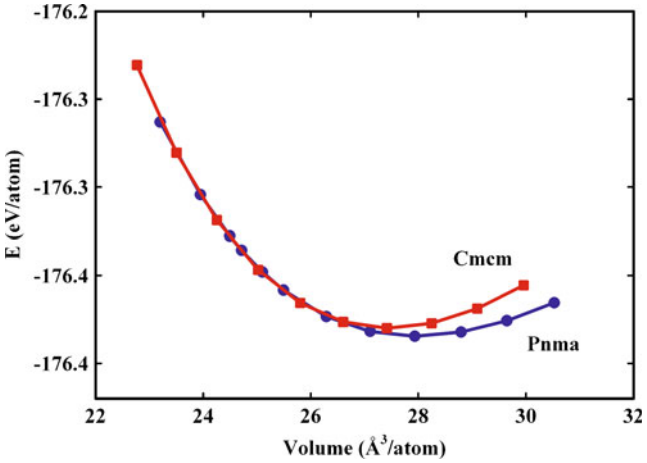

Fig. 4 The computed energies of Pnma and Cmcm phases as a function of volume

such overestimated transition pressures are anticipated. Structural phase transformations in simulations do not proceed by nucleation and growth, but instead, they occur across the entire simulation cells. So, the systems have to cross a significant energy barrier to transform from one phase to another one, and hence simulated structures have to be over pressurized in order to obtain a phase transition. Additionally, the absence of thermal motion (relaxation of the structure at constant pressure) in our simulations shifts the transitions to a higher pressure. On the other hand, the thermodynamic theorem does not take into account the possible existence of such an activation barrier separating the two structural phases and the thermal motion. Therefore, we consider the energy-volume calculations to study the stability of the *Cmcm* and *Pnma* phases. Each structure was equilibrated at several volumes and their energy-volume relations were fit to the third-order Birch Murnaghan equation of states. The energy-volume curve of the structures is presented in Fig. 4. Accordingly, the energies of the *Pnma* and *Cmcm* crystals overlap one another after a certain volume. This behavior is compatible with a continuous phase transition between these structures, which is also clearly reflected in the enthalpy calculation (see below). These findings validate our constant-pressure *ab initio* simulation.

Simple comparison of the static lattice enthalpies ($H = E_{tot} + pV$) of the *Pnma* state and the *Cmcm* state determines the transition pressure between them. The crossing of two enthalpy curves indicates a pressure-induced phase transition between these two phases. The computed enthalpy curves of the *Pnma* and *Cmcm* phases are plotted as a function of pressure in Fig. 5. The curves cross around 1.9 GPa. However, the enthalpy of both phases above 1.9 GPa practically has the same values and it is impossible to distinguish which structure is more stable than the other. This again provides clear evidence of a gradual phase transition between *Pnma* and *Cmcm*. The the *Pnma* and *Cmcm* phase change is expected to occur between 1.4 and 3.0 GPa in experiments. From the energy-volume data, we also calculate the bulk modulus of these phases. For the *Pnma* state, our bulk modulus is 31.48 GPa, which is relatively close to the experimental value of 50 GPa [19]. Since we do not have any theoretical results, comparison with the theoretical results is not possible. The bulk modulus can vary in a wide range according to the methodology of the study. The bulk modulus of the *Cmcm* phase is calculated to be 40.9 GPa.

Discussions

Our study shows that there is α-SnSe to β-SnSe phase transformation at high pressures. At high temperature, SnS and SnSe undergo second order displacive phase transition from the α-phase to the high temperature β-phase (*Cmcm*)

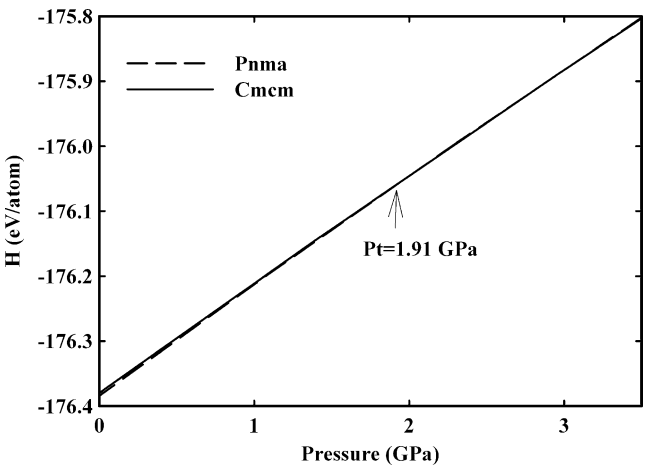

Fig. 5 Enthalpy curves of the Pnma and Cmcm phase of SnSe

at 905 K and 825 K [20, 21]. Note that the lattice constants and bond lengths of the high temperature *Cmcm* phase are comparable with those of the *Cmcm* phase formed at high pressure, indicating that both phases have the same atomic structure. The high temperature modifications β-SnSe and β-SnS crystallize in the orthorhombic structure *Cmcm* (SnSe at 825 K: a=4.410 Å, b=11.705 Å, c=4.318 Å; SnS at 905 K: a=4.148 Å, b=11.480 Å, c=4.177 Å) [21]. The bond lengths in the plane of the slab are equal to 3.06 Å and the interlayer Sn-Se bond length perpendicular the plane of slabs is 2.76 Å [21]. The simulations show the existence of the α-phase to β-phase transition at high pressure, in addition to temperature. Observing a fivefold-coordinated *Cmcm* phase formation in SnSe under pressure is not surprising due to its unique structure in which there are only two next unlike nearest neighbors at a certain distance. When the pressure is increased, each atom forms a bond with these neighbors, and the threefold-coordinated phase transforms into a fivefold-coordinated *Cmcm* state. However, the origin of the contradictory observation both in the present study and experimental is not clear but might be associated with the degree of hydrostatic pressure since the layered structures are very sensitive to shear deformations. Moreover, these similar behaviors might suggest that the phase transformation from *Pnma* to *Cmcm* can be induced in GeS at high temperatures as well and this phase transformation can also be seen in the other group IV–VI compounds because SnSe also undergoes the same phase transformation at high temperatures [20]. Certainly, further experimental and theoretical studies are needed to have a generally accepted picture about the behaviors of these compounds at high temperatures and pressures.

We also observe electronic structure of SnSe at ambient pressure and 7 GPa. The observed structural changes gave no evidence for changes of the electronic structure. Figure 6 shows the electronic density of states (EDOS) at ambient pressure and 7 GPa. At ambient conditions the compound is a semiconductor. According to the graphic (Fig. 6), there is a small shift of the Fermi level to higher energy which is interpreted as the onset of a pressure induced band gap closure. Although there are no indications for a semiconductor– semimetal transition in the pressure range studied, maybe a transition to the semimetalic state can occur at higher pressure.

Conclusions

We have studied the electronic structure of SnSe using *ab initio* constant pressure technique within a generalized gradient approximation in order to observe the pressure-induced phase transition in SnSe and predicted a structural phase transition from orthorhombic structure to another orthorhombic structure. This phase is similar to the phase formed in SnSe at high temperature. We also provide substantial information about the phase transformation from orthorhombic (*Pnma)* structure to orthorhombic structure (*Cmcm)* at the atomistic level. This phase transformation is also analyzed using the total energy calculations. The computed transition parameters and bulk properties are in agreement with experimental and theoretical data. Appling the uniaxial stress and hydrostatic pressure to the structure of SnSe, we investigate the phase transitions in SnSe. As a result of this study,

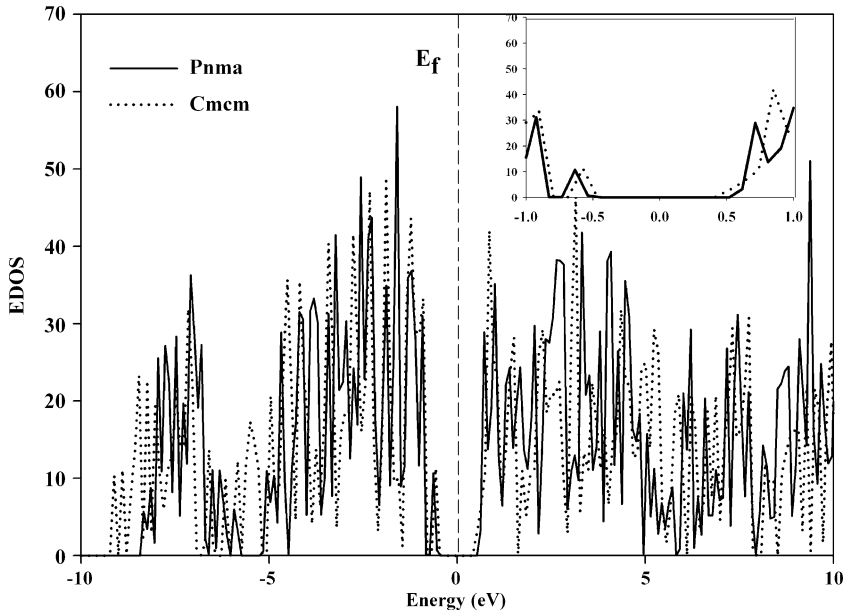

Fig. 6 Calculated electronic density of states for SnSe at 0 GPa and 7 GPa

we said that under the uniaxial stress in z-direction, at 3 GPa pressure, phase transition to *Cmcm* came about. On the other hand, under the hydrostatic pressure phase transition to *Cmcm* purely occurred at 7 GPa. So, the stress applied in z-direction is the most convenient for this material in order to obtain phase transition.

Acknowledgments We are grateful to Dr. Murat Durandurdu for his help. We are grateful to the SIESTA group for making their code publicly available.

References

1. Bhatia KL, Parthasarathy G, Gosain DP, Gopal ESR (1986) Phys Rev B 33:1492–1494
2. Hsueh HC, Vass H, Clark SJ, Ackland GJ, Crain J (1995) Phys Rev B 51:16750–16760
3. Hsueh HC, Warren WC, Vass H, Ackland GJ, Clark S, Crain J (1996) Phys Rev B 53:14806–14817
4. Onodera A, Sakamoto I, Fujii Y, Mori N, Sugai S (1997) Phys Rev B 56:7935–7941
5. Alptekin S, Durandurdu M (2010) Solid State Commun 150:870–874
6. Khvostantzev KG, Sidorov VA (1983) Phys Status Solidi B 116:83–89
7. Redon AM, Leger JM (1990) High Press Res 4:315–317
8. Durandurdu M (2005) Phys Rev B 72(4):144106
9. Okazaki A, Ueda I (1956) J Phys Soc Jpn 11:470–470
10. Abriksov NKh, Bankina VF, Poretskaya LV, Shelimova LE, Skudnova EV (1969) Semiconducting II-VI, IV-VI and V-VI compounds. Plenum, New York
11. Peters MJ, McNeil LE (1990) Phys Rev B 41:5893–5897
12. Perdew JP, Burke K, Ernzerhof M (1996) Phys Rev Lett 77:3865–3868
13. Ordejòn P, Artacho E, Soler JM (1996) Phys Rev B 53:10441–10444
14. Troullier N, Martins JM (1991) Phys Rev B 43:1993–2006
15. Monkhorst HJ, Pack JD (1976) Phys Rev B 13:5188–5192
16. Hundt R, Schön JC, Hannemann A, Jansen M (1999) J Appl Crystallogr 32:413–416
17. Knorr K, Ehm L, Hytha M, Winkler B, Depmeier W (2001) Phys Status Solidi B 233:435–440
18. Allan DR, Kelsey AA, Clark SJ, Angel RJ, Ackland GJ (1998) Phys Rev B 57:5106–5110
19. Chattopadhyay T, Werner A, von Schnering HG (1984) Rev Phys Appl 19:807–813
20. Wiedemeir H, Csillag FJ (1979) Z Kristallogr 149:17–29
21. Von Schnering HG, Wiedemeir HZ (1981) Z Kristallogr 156:143–150